

## LARGE MAGELLANIC CLOUD BAR: EVIDENCE OF A WARPED BAR

ANNAPURNI SUBRAMANIAM

Indian Institute of Astrophysics, Koramangala II Block, Sarjapur Road, Bangalore Karnataka 560-034, India

Received 2003 July 18; accepted 2003 October 9; published 2003 November 3

### ABSTRACT

The geometry of the LMC bar is studied using the dereddened mean magnitudes of the red clump stars ( $I_0$ ) from the Optical Gravitational Lensing Experiment II catalog. The value of  $I_0$  is found to vary in the east-west direction such that both the east and the west end of the bar are closer to us with respect to the center of the bar. The maximum observed variation has a statistical significance of more than  $7.6 \sigma$  with respect to the maximum value of random error. The variation in  $I_0$  indicates the presence of warp in the bar of the LMC. The warp and the structures seen in the bar indicate that the bar could be a dynamically disturbed structure.

*Subject headings:* galaxies: stellar content — galaxies: structure — Magellanic Clouds

### 1. INTRODUCTION

The Magellanic Clouds and the Milky Way are known to have experienced close encounters. These encounters would result in tidal forces that could alter the structure of the Clouds. Van der Marel & Cioni (2001), van der Marel (2001), and Weinberg & Nikolaev (2001) have studied the geometry of the LMC using Deep Near Infrared Survey of the Southern Sky and Two Micron All Sky Survey data, and they have found evidence of tidal signatures in the LMC. These studies were done on the outer regions of the LMC, at radial distances of more than  $3^\circ$ . The geometry and structure of the bar region of the LMC have not been studied in detail, although the total structure of the LMC was studied by van der Marel (2001), who detected no features and who found that the density structure of the bar region is very smooth. The interesting point that they noticed but did not give much importance to was the change in the major-axis position angle within a radial distance of  $3^\circ$ .

Olsen & Salyk (2002) studied the LMC outer regions, found evidence of a possible warp in the southwest of the LMC, and argued that the LMC plane is warped and twisted, containing features that extend up to 2.5 kpc out of the plane. The warp as found by Olsen & Salyk (2002) could have started closer to the LMC center, and it will be interesting to find the starting point of this deviation. There has been a lot of recent photometric surveys, and the Optical Gravitational Lensing Experiment II (OGLE II; Udalski et al. 2000) survey covers most of the bar region and thus is well suited for this study. We used the brightness of core helium-burning red clump stars in the bar region of the LMC as a probe of the bar structure. The difference in the dereddened mean magnitude of the red clump stars is used as a differential distance indicator. The technique used here is identical to the one used by Olsen & Salyk (2002). We look for evidence of tidal interaction in the bar region, like the presence of a warp, within a radial distance of  $3^\circ$ .

### 2. DATA SELECTION AND ESTIMATION OF DEREDDENED MEAN MAGNITUDE ( $I_0$ )

The OGLE II survey (Udalski et al. 2000) consists of photometric data of 7 million stars in  $B$ ,  $V$ , and  $I$  passbands in the central  $5.7 \text{ deg}^2$  of the LMC. The data are presented for 21 regions, which are located within  $2^\circ.5$  from the optical center of the LMC. Initially, the total observed region was divided into 336 sections of size  $7.1 \times 7.1 \text{ arcmin}^2$  each. The red clump

stars are identified using an  $I$  versus  $(V-I)$  color-magnitude diagram (CMD), and, on average, 7000 red clump stars were identified per region.

The data suffer from the incompleteness problem due to crowding effects, and the incompleteness in the data in the  $I$  and  $V$  passbands is tabulated in Udalski et al. (2000). The frequency distribution of red clump stars in each CMD is estimated in both  $I$  magnitude and  $(V-I)$  color after correcting for the data incompleteness, using a bin size of 0.015 mag for  $(V-I)$  color and 0.025 mag in  $I$  magnitude. These distributions are fitted with the Gaussian+quadratic function, similar to Olsen & Salyk (2002). The distributions are fitted using a nonlinear least-square fits, to obtain the best-fitting parameters when the  $\chi^2$ -value is minimum. The parameters estimated are the peak of the function, the error in the estimated peak value, the width of the profile, and the goodness of fit. The above-described area is chosen so as to have a good number of stars for the fit. On the other hand, the choice of area should not affect the conclusions derived here. Therefore, two more data sets were created by dividing the observed area into 672 sections ( $3.56 \times 7.1 \text{ arcmin}^2$ ) and 1344 sections ( $3.56 \times 3.56 \text{ arcmin}^2$ ), and the frequency distribution and the fit parameters were estimated for these data also. The number of red clump stars in these area bins also scales like the area. In order to estimate the goodness of fit, the reduced  $\chi^2$ -values were estimated. After rejecting the distributions with very high  $\chi^2$ -values, the average values of reduced  $\chi^2$  for the fit of the  $I$ -magnitude distribution are 1.68, 1.60, and 1.59, and those for the  $(V-I)$  distribution are 1.65, 1.49, and 1.39, for the largest, medium, and smallest area bin, respectively. It can be seen that the choice of area does not affect the shape of the distribution very much or the derived parameters. As the average value of the reduced  $\chi^2$  is found to be minimal for the smallest area bin, the smallest area bins are chosen for further analysis. A typical frequency distribution of red clump stars in  $I$  and  $(V-I)$  magnitudes is shown in Figure 1. The reduced  $\chi^2$ -value of the fit and the estimated value of the peak and its error are also indicated in the figure. For further analysis, we restrict the data points with a reduced  $\chi^2$ -value of less than 2.6, which reduces the number of regions to 1191.

The peak values of the color,  $(V-I)$  mag at each location, are used to estimate the reddening. The reddening is calculated using the relation  $E(V-I) = (V-I)_{\text{obs}} - 0.92 \text{ mag}$ . The intrinsic color of the red clump stars is assumed to be 0.92 mag (Olsen & Salyk 2002). The interstellar extinction is estimated by  $A_V = 1.4E(V-I)$  (Schlegel, Finkbeiner, & Davis 1998). Af-

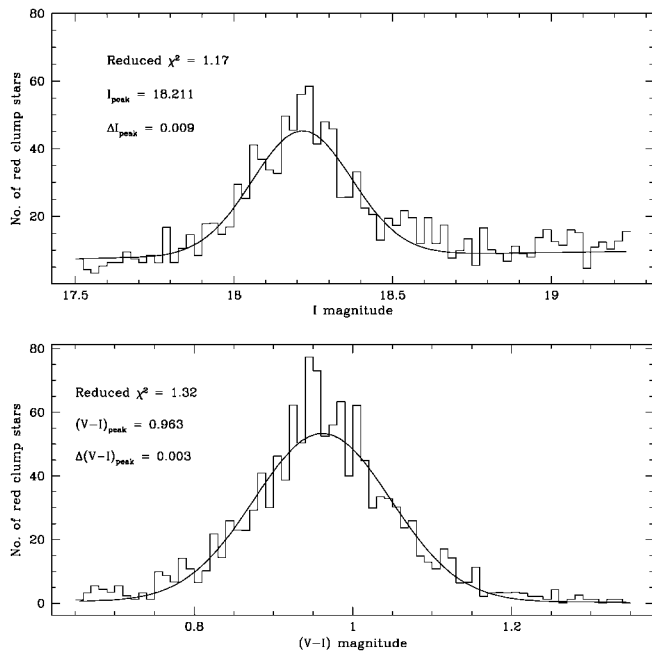


FIG. 1.—Luminosity function of red clump stars plotted against  $I$  magnitude and  $(V-I)$  color. The reduced  $\chi^2$ -value of the fit of the function to the distribution and the estimated values of the peak and its error are indicated. These data are obtained within a area of  $3.56 \times 3.56$  arcmin<sup>2</sup> centered at R.A. =  $5^{\text{h}}32^{\text{m}}45^{\text{s}}$  and decl. =  $-70^{\circ}25'37''$ .

ter correcting the mean  $I$  magnitude for interstellar extinction,  $I_0$  is estimated for each region.

The error in the estimation of the peak values of the  $I$  and  $(V-I)$  distribution is shown as a function of right ascension in Figure 2. Since the data spans about  $12^{\circ}$  in right ascension and since the span in declination is only about  $2^{\circ}$ , the error variations are shown as a function of right ascension. In general, most of the data points have  $\Delta(V-I)_{\text{peak}} \leq 0.005$  mag and  $\Delta I_{\text{peak}} \leq 0.02$  mag, and about 2% of the points have slightly higher errors. We have chosen regions that have errors less than or equal to the values indicated above, for further analysis. Since the random error in the estimation of  $I_0$  has contributions from  $\Delta(V-I)_{\text{peak}}$  and  $\Delta I_{\text{peak}}$ ,  $\Delta I_0$  can be estimated as  $\Delta I_0^2 = [\Delta(V-I)_{\text{peak}}^2 + (\Delta I_{\text{peak}})^2]$ . If we consider the maximum errors in the peak values, which are  $\Delta(V-I)_{\text{peak}} = 0.005$  and  $\Delta I_{\text{peak}} = 0.02$ , then the maximum random error in  $I_0$  is  $\Delta_{\text{max}} I_0 = 0.021$  mag. Another factor that can contribute to the total error is the reddening. The  $E(V-I)$  reddening values of eight adjacent regions were averaged, and the standard deviation in the mean reddening was estimated. This value of the standard deviation in the reddening is also plotted in Figure 2. The average reddening is found to be  $E(V-I) = 0.081 \pm 0.004$  mag, and these values as a function of right ascension are shown in the bottom panel of Figure 2. It can be seen that  $\Delta_{\text{max}} E(V-I) = 0.029$  mag. The rejection criteria based on the errors in the peak value, as mentioned above, remove the regions that show higher deviation in reddening also. Hence, after the rejections, the  $\Delta_{\text{max}} E(V-I)$  is found to be 0.02 mag. A systematic error in the estimation of  $I_0$  can arise from  $\Delta E(V-I)$ . If one considers 0.004 mag as the standard deviation in the reddening estimate, then the total error due to random error as well as systematic effects is 0.021 mag, which is the same as  $\Delta_{\text{max}} I_0$ . If we take a value of 0.02 mag as the upper limit in the standard deviation in reddening, then the

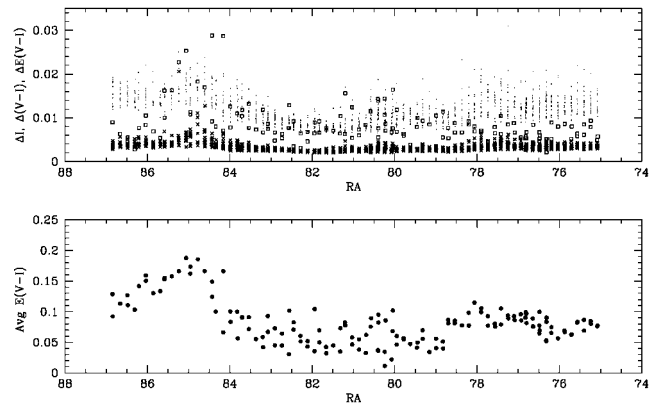


FIG. 2.—*Top panel*: Error in the estimation of the peak of  $I$  magnitude (*dots*) and  $(V-I)$  color (*crosses*) of the red clump luminosity function shown as a function of right ascension for 1191 regions. The dispersion in the reddening  $E(V-I)$  is indicated as open squares. *Bottom panel*: Average reddening  $E(V-I)$  shown as a function of right ascension.

maximum total error due to all three sources is 0.029 mag. The zero-point error and photometric errors are not included here since they are almost the same for the entire data, the data being homogeneous.

### 3. RESULTS AND DISCUSSION

The two-dimensional figure of the region studied here is shown in Figure 3, where the variation in  $I_0$  is shown as a function of right ascension and declination. The farthest points have  $I_0 > 18.24$  mag, and the closest points have  $I_0 < 18.08$  mag. This corresponds to a net difference of more than 0.16 mag. This value is more than 7.6 times the maximum random error and more than 5.6 times the maximum total error. Hence, the net variation in the dereddened mean red clump magnitudes is statistically significant.

At locations R.A. =  $79^{\circ}5$  and decl. =  $-69^{\circ}6$  and R.A. =  $84^{\circ}5$  and decl. =  $-70^{\circ}$ , the  $I_0$ -values are higher, indicating that these regions are located at a larger distance. The regions in between the above points are closer to us. The easternmost regions are closest, as indicated in the figure. At R.A. =  $84^{\circ}5$ , another feature that can be noticed is that along the declination axis, where there is a change in the relative distance. This is such that the northern regions are farther and the southern regions are closer. The difference in  $I_0$  is more than 3.8 times the  $\Delta_{\text{max}} I_0$ . The center of the LMC is taken to be R.A. =  $05^{\text{h}}19^{\text{m}}38^{\text{s}}0$ , decl. =  $-69^{\circ}27'5''2$  (2000.0; de Vaucouleurs & Freeman 1973). Then the center lies near the fainter  $I_0$  points located around R.A. =  $79^{\circ}5$ . Thus, the regions westward of the center are also found to be closer.

In order to study the variation of  $I_0$  along the right ascension,  $I_0$ -values along declination are averaged, and a plot of  $\text{avg}(I_0)$  versus right ascension is shown in Figure 4. The error bars indicate the deviation in  $I_0$  along the declination, for a given right ascension. It can be seen that there are variations in the  $I_0$  magnitude along the bar. The center of the LMC is shown as an open circle. The most striking feature is the wavy pattern in  $I_0$ . The eastern side of the bar is closer to us, when compared with the bar region near the center. The western side is also closer to us. We see an M-type variation in  $I_0$  along the right ascension. Thus, the features indicate that the bar of the LMC is warped. It would be interesting to find the relative

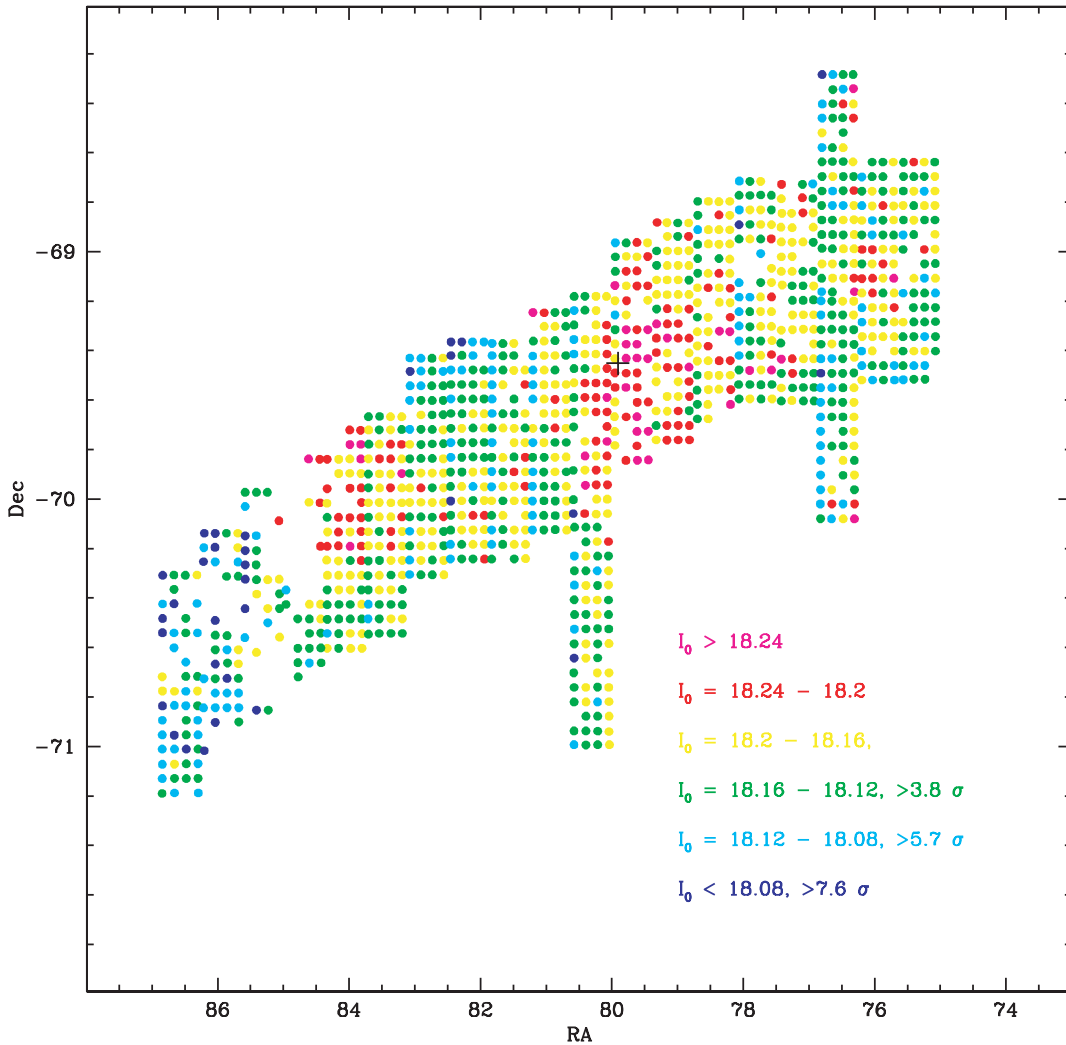


FIG. 3.—Two-dimensional plot of the dereddened mean red clump magnitude,  $I_0$ , for 1123 regions. The color code used is such that, from magenta to blue, magenta indicates regions that are the farthest, and blue indicates regions that are closest. The statistical significance of the  $I_0$  bins with respect to maximum random error is also indicated. The black plus sign shows the location of the center of the LMC.

inclinations of the disk and the bar since these would help us to estimate their locations. The geometry of the bar based on the  $I_0$  variation will be presented in another paper, which is in preparation. It would be ideal to use the photometric data of the LMC stars from other surveys, like the MACHO survey, to estimate the disk parameters.

The structure of the bar as derived here is delineated by stars belonging to the red clump population. The techniques used in this study were used earlier by many studies (van der Marel 2001; Udalski et al. 1998; van der Marel & Cioni 2001). The data used here have been used by Udalski et al. (1998) to estimate the distance to the LMC, but they have not used it to study the relative distances within the LMC. The reddening is found to be almost a constant along the bar, except in the east end; therefore, the magnitude variation is not an imprint of reddening in the bar. The variation in the red clump luminosity could also be due to the age and metallicity difference, rather than due to the relative distance. The study by Subramaniam & Anupama (2002) on the local stellar population of nova regions found no major difference in the population of the

intermediate-age stars in the bar region. This is again supported by the findings of Olsen & Salyk (2002) and van der Marel & Cioni (2001). Hence, the variation seen in  $I_0$  magnitude is mainly due to the geometry of the bar. The estimates of the self-lensing optical depth in the LMC appear to be too low to account fully for the entire microlensing optical depth (Gould 1995). This kind of a structure in the bar would contribute to more optical depth within the LMC, which can increase the self-lensing within the LMC.

The LMC bar is thus found to show structures. The presence of warp in the bar indicates that the bar is dynamically disturbed. Since the bar is located well within the tidal radius of the LMC, the tidal effects due to the LMC-SMC-Galaxy interaction may not be the cause of the disturbance. On the other hand, if the bar is not aligned with the disk, then the disk can induce perturbations on the bar. This in turn can create structures in the bar. In order to explain the LMC microlensing events, Zhao & Evans (2000) proposed the bar to be an unvirialized structure, which is slightly misaligned with and offset from the LMC disk. Zhao & Evans (2000) also claimed that

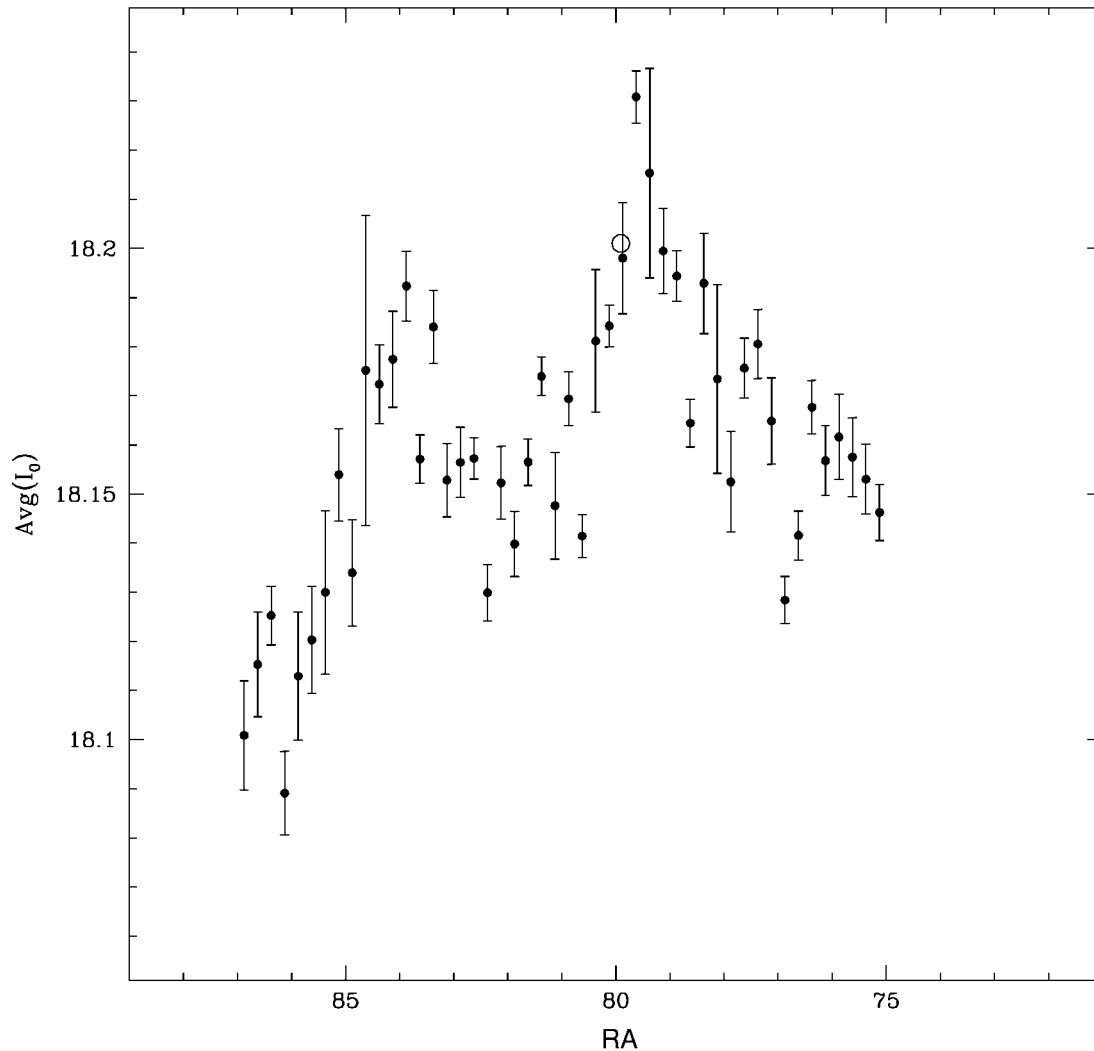


FIG. 4.—Average of the  $I_0$  along the declination estimated for various right ascensions. The value  $\text{avg}(I_0)$  is shown against the right ascension. The error indicates the scatter in  $I_0$  along the declination. The open circle shows the location of the center of the LMC.

the interactions of the Magellanic Clouds with the Galaxy could be responsible for the misalignments and displacements of the bar with respect to the disk. Therefore, it is necessary to find out the geometry of the bar and the disk, which would throw light on the source of perturbations in the bar.

I thank Ram Sagar, Uma Gorti, G. C. Anupama, and Kiran Jain for helpful discussions. I also thank the referee for his comments that improved the presentation of this Letter.

#### REFERENCES

- de Vaucoulers, G., & Freeman, K. C. 1973, *Vistas Astron.*, 14, 163  
 Gould, A. 1995, *ApJ*, 441, 77  
 Olsen, K. A. G., & Salyk, C. 2002, *AJ*, 124, 2045  
 Schlegel, D. J., Finkbeiner, D. P., & Davis, M. 1998, *ApJ*, 500, 525  
 Subramaniam, A., & Anupama, G. C. 2002, *A&A*, 390, 449  
 Udalski, A., Szymański, M., Kubiak, M., Pietrzyński, G., Soszyński, I., Woźniak, P., & Żebruń, K. 2000, *Acta Astron.*, 50, 307  
 Udalski, A., Szymański, M., Kubiak, M., Pietrzyński, G., Woźniak, P., & Żebruń, K. 1998, *Acta Astron.*, 48, 1  
 van der Marel, R. P. 2001, *AJ*, 122, 1827  
 van der Marel, R. P., & Cioni, M.-R. 2001, *AJ*, 122, 1807  
 Weinberg, M., & Nikolaev, S. 2001, *ApJ*, 548, 712  
 Zhao, H. S., & Evans, N. W. 2000, *ApJ*, 545, L35